NJC

Check for updates

A new multi-analyte fluorogenic sensor for efficient detection of Al^{3+} and Zn^{2+} ions based on ESIPT and CHEF features†

Lakshman Patra, Sangita Das, Saswati Gharami, Krishnendu Aich and Tapan Kumar Mondal [ID] *

The fluorogenic chemosensor 3-(((2-hydroxy-4-methylphenyl)imino)methyl)-[1,1′-biphenyl]-4-ol (H$_2$L) efficiently detects Zn^{2+} and Al^{3+} ions and subsequently fluoride ion in methanol–water (4/1, v/v, pH = 7.2) solution. The probe itself is non-emissive but upon treatment with Al^{3+} and Zn^{2+}, it exhibits high fluorescence emission at two different wavelengths of 546 nm and 529 nm, respectively. Both excited-state intramolecular proton transfer (ESIPT) and chelation enhanced fluorescence (CHEF) processes play important roles in the enhancement of fluorescence intensity. Chelation of Zn^{2+} and Al^{3+} with the probe (H$_2$L) inhibits C=N isomerization and ESIPT which consequently enhances the emission intensity. The emission intensity of H$_2$L–Al^{3+} is selectively quenched upon titration with F$^-$ anions. The structure of the probe is confirmed by the single crystal X-ray diffraction method. The electronic structure and sensing mechanism of the probe (H$_2$L) are supported by density functional theory (DFT) and time-dependent density functional theory (TDDFT).

Introduction

There are many versatile applications of organic probes in different fields such as chemistry, biology and the environment for the selective detection of chemical and biological species.[1,2] The detection mechanism of most chemosensors is based on metal–ligand coordination,[3–5] electrostatic interactions,[6–8] hydrogen bonding,[9–11] van der Waals forces[12] and hydrophobic interactions.[13–15] Among them, the metal–ligand chelation enhanced fluorescence (CHEF) approach is most exciting as visualization and imaging both are possible due to the fluorescence turning on after interaction with the guest analyte. Chemosensors with different responses towards different analytes are highly desirable. But it is challenging to develop such a probe. So there is great research interest in this field in recent times.

Aluminum is the third most abundant element in the biosphere, and nearly 8% of the total mineral component is aluminum. It is widely used in our daily life such as for food packaging, drinking water supplies, cookware, deodorant, bleached flour, antiperspirants, antacids and the manufacturing of cars and computers.[16–18] Although it is extensively used in our modern life, it

is harmful to both our environment and biological system. Al(III) leaches from soil during acid rain, deadly for growing plants.[19–22] Abnormal concentrations of aluminum in our body cause various dangerous diseases such as Alzheimer's, Parkinson's disease, bone softening, impaired lung function, fibrosis, chronicrenal failure *etc.*[23–26] According to the WHO, regulation of the maximum Al(III) present in drinking water should be up to 7.42 μM and daily intake should be less than 3–10 mg.[27–29] Therefore, due to environmental and health concerns, it is necessary to develop a chemosensor for the detection of Al(III).

On the other hand, zinc is the second most abundant element in the human body.[30] It plays an important role in gene transcription, cellular metabolism, immunological functions and signaling processes in the brain.[31–33] Although it is an essential trace element in the human body, excessive amounts of this metal can cause several neurological disorders such as Alzheimer's and Parkinson's diseases.[34,35] Up to 8–11 mg per day of Zn(II) intake is tolerable for maintaining good health.[36] In the presence of higher concentrations of zinc in the human body, other essential trace elements such as iron, copper *etc.* cannot work properly.[37]

Fluoride sensing is also one of the most attractive fields of research nowadays as it has immense potential in biology and chemistry.[38,39] Excessive amounts of fluoride can cause several diseases in our body such as urolithiasis, osteoporosis, stomach ulcers or even cancer.[40–43] There are very few chemosensors which can detect both Al(III) and Zn(II) and sequentially fluoride anions as it

Department of Chemistry, Jadavpur University, Kolkata 700032, India.
E-mail: tapank.mondal@jadavpuruniversity.in

is challenging due to the weak coordination ability of Al(III) compared to any 3d metal ions. Dr Congbin Fan and Dr Shouzhi Pu have reported a chemosensor which can detect Al(III) as well as Zn(II).[44]

Herein, we have synthesized a simple, cost-effective, dual sensing probe for detection of Al(III) and Zn(II) metals and subsequently F⁻ anions based on ESIPT and CHEF sensing mechanisms. One can clearly visualize the color changes on addition of the ions by the naked eye in order to confirm the sensing protocol with the aid of this newly developed probe.

Results and discussion

Synthesis of the probe (H$_2$L)

The probe is synthesized by an inexpensive and simple process. First, formylation of 4-phenylphenol results in 4-hydroxy-[1,1′-biphenyl]-3-carbaldehyde. Then a 1:1 Schiff base condensation reaction of the aldehyde and 2-amino-4-methylphenol in ethanol solvent under reflux conditions yields the desired probe (H$_2$L) (Scheme 1). H$_2$L is characterized by several spectroscopic techniques, *viz.*, ^{1}H NMR, ^{13}C NMR, mass spectrometry and elemental analysis (Fig. S19–S22, ESI†). In addition, the structure of the probe is confirmed in the solid state by the single crystal X-ray diffraction method. The ORTEP plot of the probe (H$_2$L) is shown in Fig. 1. A summary of the crystallographic data is given in Table S3 in the ESI.† The compound crystallizes in orthorhombic crystal system with the *Pca*2$_1$ space group. Some selected bond distances are summarized in the caption of Fig. 1.

Sensing studies of H$_2$L

UV-vis study. The UV-vis spectrum of the probe (H$_2$L) exhibits absorption bands at 255 nm, 359 nm and 470 nm in
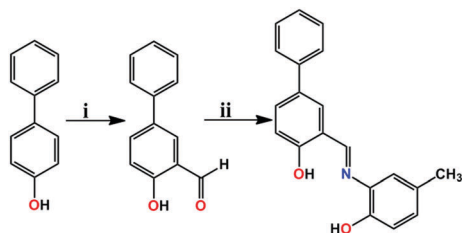
Scheme 1 Synthesis of the probe (H$_2$L). *Reagents and conditions*: (i) TFA, hexamine, 90° – 100 °C, reflux, 6 h; (ii) 2-amino-4-methylphenol, reflux, 6 h.
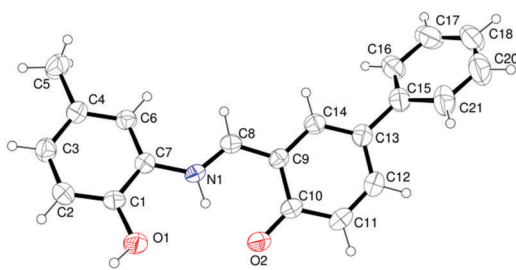
Fig. 1 ORTEP plot of the organic probe H$_2$L (O1–C1, 1.356(5) Å; O2–C10, 1.297(5) Å; N1–C7, 1.411(5) Å; N1–C8, 1.305(5) Å; C1–C7, 1.383(5) Å; C8–C9, 1.401(5) Å and C9–C10, 1.437(5) Å).

CH$_3$OH/H$_2$O (4/1, v/v, pH = 7.2) solution. Upon titration of H$_2$L (20 μM) in CH$_3$OH/H$_2$O (4/1, v/v, pH = 7.2) with different metal ions such as Ca^{2+}, Cr^{3+}, Co^{2+}, Mn^{2+}, Fe^{3+}, Cd^{2+}, Cu^{2+}, Hg^{2+}, Ni^{2+}, Na$^+$, Pb^{2+}, Al^{3+} and Zn^{2+} (40 μM), no significant changes are observed except for Al^{3+} and Zn^{2+} (Fig. 2 and Fig. S5, ESI†). The absorption bands at 359 nm and 470 nm disappear, a new band appears at 435 nm, and the band at 255 nm shifts to 245 nm. To understand the effect of anions on the absorption bands of the probe (H$_2$L), UV-vis spectra are also taken in the presence of various anions. The absorption bands of the probe remain almost unaltered upon titration with various anion solutions (Fig. S6, ESI†).

Fluorescence study. Emission properties of the free probe (H$_2$L) and in the presence of different ions are studied to explore the sensing properties. The free receptor has a very low emission property; it exhibits very weak emission at 565 nm with a very low quantum yield (ϕ = 0.00215) upon excitation at 400 nm. Upon addition of Al^{3+} solution (40 μm) to the receptor solution (20 μm), the emission intensity significantly increased with a small blue shift at 545 nm (λ_{ex} = 400 nm) (Fig. 3), and the quantum yield (ϕ) increased to 0.212. On the other hand, titration of the receptor (20 μm) with Zn^{2+} (40 μm) in CH$_3$OH/H$_2$O (4/1, v/v, pH = 7.2) solution results in significant enhancement of the emission intensity at λ_{max} 529 nm (ϕ = 0.041) (Fig. 4). To check the selectivity of the receptor, emission properties are also studied in the presence of other metal ions such as Ca^{2+}, Cr^{3+}, Co^{2+}, Mn^{2+}, Fe^{3+}, Cd^{2+}, Cu^{2+}, Hg^{2+}, Ni^{2+}, Na$^+$,
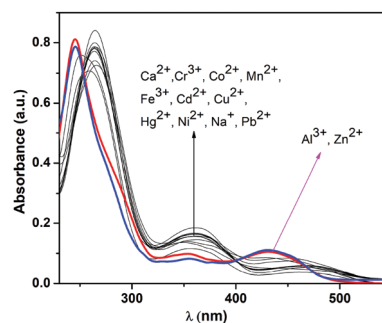
Fig. 2 Change in the absorption spectrum of H$_2$L (20 μM) upon addition of different cations (40 μM) in CH$_3$OH/H$_2$O (4/1, v/v, pH = 7.2) solution.
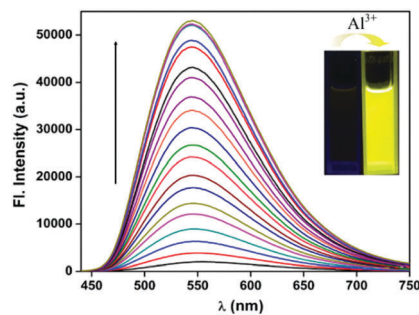
Fig. 3 Change in the emission intensity of H$_2$L (20 μM) upon gradual addition of Al^{3+} (0–40 μM) in CH$_3$OH/H$_2$O (4/1, v/v, pH = 7.2) solution. Inset: The visual effect of addition of Al^{3+} to H$_2$L under UV light. λ_{ex} = 400 nm.
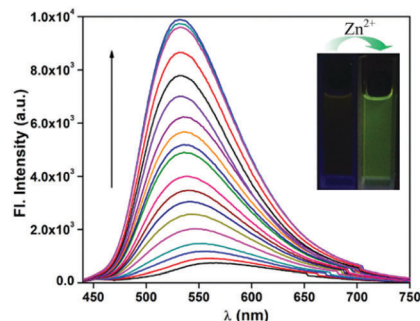
Fig. 4 Change in the emission spectrum of H_2L (20 μM) upon gradual addition of Zn^{2+} (0–40 μM) in CH_3OH/H_2O (4/1, v/v, pH = 7.2) solution. Inset: The visual effect of addition of Zn^{2+} to H_2L under UV light. λ_{ex} = 400 nm.
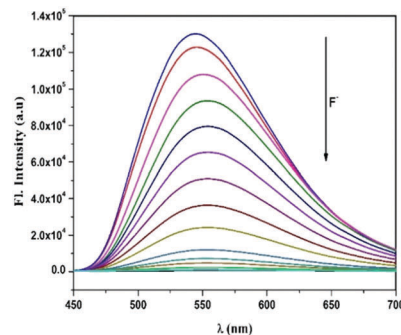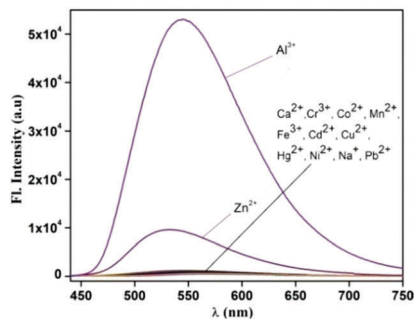

Fig. 5 Change in the emission spectrum of H_2L (20 μM) upon addition of different cations (40 μM) in CH_3OH/H_2O (4/1, v/v, pH = 7.2) solution.

and Pb^{2+} but the emission intensity remains almost unaltered (Fig. 5 and Fig. S2, ESI†). Therefore, the increase of emission intensity of the receptor (H_2L) is very selective towards Al^{3+} and Zn^{2+} ions.

To understand the effect on the emission intensity in the presence of anions, the fluorescence spectra are taken with addition of various anion solutions to the receptor (H_2L). But no significant changes in the emission property of the probe are observed (Fig. S7, ESI†). Although the probe is silent to various anions, it can be used as a sequential chemosensor for fluoride ions. Upon titration of H_2L–Al^{3+} solution (20 μm) (mixture of H_2L and Al^{3+} solution in 4:1 methanol–water solvent) with fluoride ions (40 μm), the emission intensity decreases gradually due to the formation of the free receptor and a very stable AlF_3 compound (Fig. 6). In the presence of other anions no significant changes in the fluorescence intensity of the H_2L–Al^{3+} solution are observed. Again, to illustrate the reversibility of the interaction of H_2L with Zn^{2+}, H_2L–Zn^{2+} solution (20 μm) (mixture of H_2L and Zn^{2+} solution in 4:1 methanol–water solvent) is titrated with EDTA solution (40 μm). Upon gradual addition of EDTA solution, the emission intensity of the H_2L–Zn^{2+} complex gets quenched to the free probe (H_2L) emission intensity (Fig. S8, ESI†).

A plot of the change in the fluorescence intensity of the receptor (H_2L) at 546 nm with increasing concentration of Al^{3+} is shown for quantitative study of sample solutions (Fig. S9, ESI†).

Fig. 6 Change in the emission spectrum of the H_2L–Al^{3+} complex (20 μM) upon gradual addition of F^- (0–40 μM) in CH_3OH/H_2O (4/1, v/v, pH = 7.2) solution, λ_{ex} = 400 nm.

The emission intensity increases linearly with the concentration of Al^{3+} which implies that H_2L is applicable for quantitative detection. The same experiment is also carried out for Zn^{2+} which shows its compatibility towards quantitative detection (Fig. S10, ESI†).

The limit of detection (LOD) of the probe (H_2L) towards the guest analytes is calculated from the fluorescence titration data using the equation LOD = $K \times$ SD/S where SD and S stand for the standard deviation and the slope of the linear response curve respectively. LOD is found is to be as low as 2.24×10^{-7} M, 4.1×10^{-8} M and 3.7×10^{-8} M for Al^{3+}, Zn^{2+} and F^- respectively (Fig. S9–S11, ESI†). Thus the present probe (H_2L) can detect these ions even at very minute levels. To illustrate the efficiency and selectivity of the present probe (H_2L) towards Al^{3+} and Zn^{2+} ions the limit of detection and solvent systems of some reported fluorescence probes are summarized in Table S4 (ESI†). Association constants (K_a) of the probe for Al^{3+} and Zn^{2+} are calculated as 0.71×10^5 M^{-1} and 0.74×10^4 M^{-1} respectively from fluorescence titration using the Benesi–Hildebrand equation. The Job plot confirms the 1:1 complexation of H_2L with both Al^{3+} and Zn^{2+} ions in solution (Fig. S12 and S13, ESI†).

The pH dependence of the receptor for the sensing of metal ions is also studied. Solutions of H_2L with Al^{3+} and Zn^{2+} are prepared separately in CH_3OH–H_2O (4:1, v/v) solution at different pH values (2–12) and the fluorescence intensity is measured. For the free receptor, the emission of the solution remains almost unaltered with an increase in pH. Both the H_2L–Al^{3+} and H_2L–Zn^{2+} solutions show the highest emission at pH 7.0 implying the maximum sensing ability of the probe at neutral pH conditions (Fig. 7).

TRPL study. A nanosecond time resolved fluorescence study is carried out to examine the exited state behaviour of the free receptor, H_2L, and in the presence of Al^{3+} and Zn^{2+}. The fluorescence lifetime decay profile diagram is obtained by using a mono exponential function for H_2L–Al^{3+} and a bi-exponential function for H_2L–Zn^{2+} with acceptable χ^2 values (Fig. 8). The receptor has a very low fluorescence lifetime in CH_3OH–H_2O (4:1, v/v) but after complexation with metal ions, the lifetime significantly increases. The lifetime (τ) of the H_2L–Zn^{2+} complex is found to be 2.30 ns (χ^2 = 1.05) which is 0.70 ns greater than the free receptor. The fluorescence lifetime of H_2L–Al^{3+} (τ = 5.02 ns) is also enhanced significantly and is
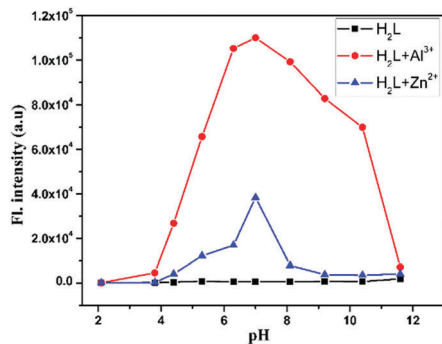
Fig. 7 Fluorescence response of H_2L (-■-■-), H_2L–Al^{3+} (-●-●-) and H_2L–Zn^{2+} (-▲-▲-) as a function of pH in CH_3OH/H_2O (4/1, v/v); pH is adjusted by using aqueous solutions of 1 M HCl or 1 M NaOH.
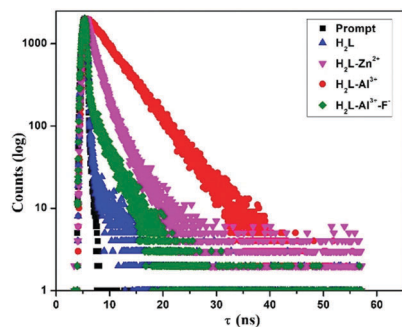
Fig. 8 Time-resolved fluorescence decay of H_2L (▲▲▲), H_2L–Al^{3+} (●●●), H_2L–Zn^{2+} (▼▼▼), H_2L–Al^{3+}–F^- (◆◆◆) and prompt (■■■) (λ_{ex} = 370 nm).

even found to be greater than that of the H_2L–Zn^{2+} complex. After sequential addition of F^- to the H_2L–Al^{3+} the lifetime decreases to τ = 1.67 ns (χ^2 = 1.04) which is nearly the same as that of the free receptor lifetime value (τ = 1.60 ns, χ^2 = 1.05). The studies suggest that the free receptor, H_2L, has a low fluoroscence lifetime due to the ESIPT effect. After complexation with metal ions (Zn^{2+} and Al^{3+}), structural rigidity appears in the receptor and it shows the CHEF effect suppressing ESIPT. Due to the CHEF process, complexes exhibit higher fluorescence emission with enhanced lifetime values. After addition of fluoride ions to the H_2L–Al^{3+}, AlF_3 precipitates out and the probe, H_2L, becomes free. So the lifetime of the H_2L–Al^{3+} decreases to 1.67 ns. Radiative rate constant K_r and total non radiative rate constant K_{nr} have been calculated using the equations $\tau^{-1} = K_r + K_{nr}$ and $K_r = \phi_f/\tau$ (Table S1, ESI†).

Competition study. For a best chemosensor, sensing of its guest analyte should be largely unaffected by the presence of competitive species. The interference experiment for the detection of Al^{3+} and Zn^{2+} is also accomplished in the presence of other competing metal ions such as Ca^{2+}, Cr^{3+}, Co^{2+}, Mn^{2+}, Fe^{3+}, Cd^{2+}, Cu^{2+}, Hg^{2+}, Ni^{2+}, Na^+, and Pb^{2+}. The competition study shows that all the competitive metal ions do not interfere with the sensing and H_2L exhibits its ability for selective detection of Al^{3+} and Zn^{2+} separately (Fig. S16 and S17, ESI†). In a natural sample, both Al^{3+} and Zn^{2+} may be present. So, a
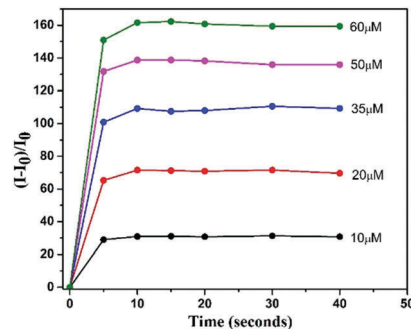

Fig. 9 Fluorescence response of H_2L (20 μM) with different concentrations of Al^{3+} (10–60 μM) at different times in CH_3OH/H_2O (4/1, v/v, pH = 7.2).

sample solution containing both Al^{3+} and Zn^{2+} ions is tested by the receptor. The experiment shows that the receptor (H_2L) prefers to interact with Al^{3+} and shows its sensitivity compared to its interaction with Zn^{2+} ions.

Time course of sensing. The time required for detection of Al^{3+} and Zn^{2+} is studied by measuring the fluorescence intensity change with time of various ion concentrations in CH_3OH–H_2O (4:1, v/v) solvent. A fast sensing probe is always necessary for practical applications. The measurement of emission intensity is started after 5 seconds of the addition of guest ions to the receptor solution. The experiment shows that the emission intensity instantly reaches the maximum value both for Al^{3+} and Zn^{2+} ions (Fig. 9 and 10). Moreover, the fast complexation process induced the CHEF and prohibited the ESIPT process.

Sensing mechanism. The weak fluorescence intensity of the receptor H_2L is probably due to intramolecular proton transfer (ESIPT) and C=N isomerization processes in the free state of the probe (Fig. S18, ESI†). Both the processes are prohibited due to the coordination with the metal ions. On the other hand due to the chelation enhanced fluorescence (CHEF) effect the emission intensity increased significantly in the complexes. The interaction between the receptor and the ions is investigated by the Job plot and ^1H NMR analysis. In methanol–water solvent, the Job plot exhibits 1:1 complexation of H_2L with Al^{3+} and Zn^{2+} ions (Fig. S12 and S13, ESI†). The ^1H NMR spectrum of the probe in DMSO-d_6 exhibits phenolic-OH and –NH proton
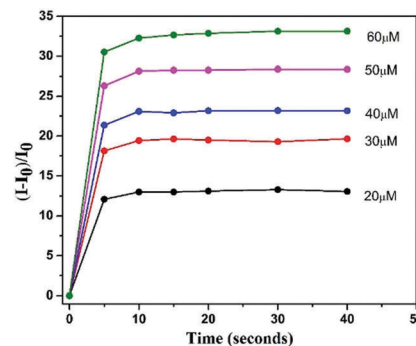

Fig. 10 Fluorescence response of H_2L (20 μM) with different concentrations of Zn^{2+} (20–60 μM) at different times in CH_3OH/H_2O (4/1, v/v, pH = 7.2).
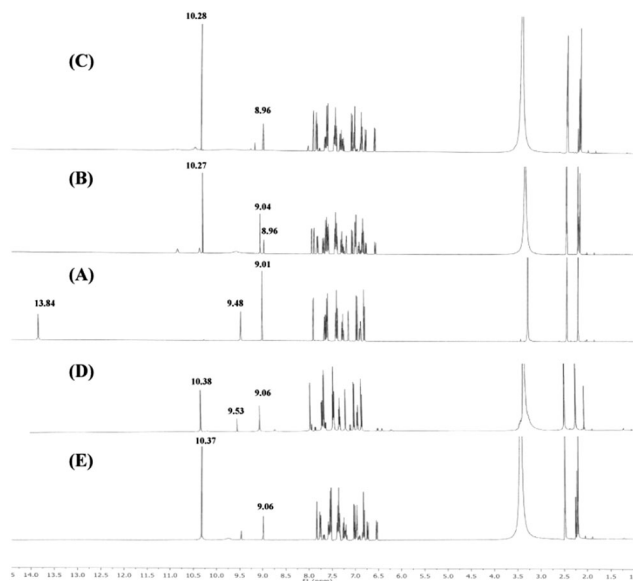
Fig. 11 Partial ^{1}H NMR (400 MHz) spectra of (A) H_2L, (B) H_2L + Al^{3+} (1 equiv.), (C) H_2L + Al^{3+} (2 equiv.), (D) H_2L + Zn^{2+} (1 equiv.) and (E) H_2L + Zn^{2+}(2 equiv.) in DMSO-d_6.

signals at δ 13.84 and δ 9.48 respectively which disappear upon interaction with Al^{3+} and Zn^{2+}. This suggests dissociation of phenolic-OH and –NH protons during coordination with metal ions. The singlet peak of the =CH–N proton appeared at the downfield region in the complexes (Fig. 11).

Practical application. For on-site visual detection of Al^{3+} and Zn^{2+}, a paper strip test is performed. Filter paper strips are prepared by immersing filter paper into a methanol solution of the receptor H_2L (0.1 mM) and drying it in air. A fluorescence colour change was observed in both cases of Al^{3+} and Zn^{2+} when strips are dipped in aqueous solutions (0.1 mM) of these ions separately and dried. This change of emission colour can be easily visualised by the naked eye when exposed to UV light (Fig. 12). The distinct colours of the paper strips containing H_2L for Al^{3+} and Zn^{2+} ions under UV light help us to easily distinguish them. The detection limit using paper strips is not as much as the solution phase and was found to be 0.1 mM.

Computational study. A theoretical calculation is performed to clarify the sensing mechanism of the probes in the ground state as well as to gain insight into the optimized geometries of the free probes and in the complexes (Fig. S30, ESI†). Contour plots of selected molecular orbitals of H_2L, H_2L–Al^{3+} and H_2L–Zn^{2+} are shown in Figs. S31, S32 and S33 (ESI†). The HOMO–LUMO

energy gap in the free receptor (2.98 eV) is significantly increased in the H_2L–Al^{3+} (3.22 eV) and H_2L–Zn^{2+} (3.24 eV) complexes. The changes in the HOMO–LUMO energy gap are also reflected in the calculated electronic transitions by the TDDFT/B3LYP method (Table S2, ESI†).

Conclusions

Herein, we have synthesized a cost-effective chemosensor which can detect Al^{3+} and Zn^{2+} ions very rapidly (within 5 seconds). It can also be used as a subsequent chemosensor for F^- anions. In Al^{3+} and Zn^{2+} complexes of the receptor, ESIPT is inhibited and the CHEF effect enhances the fluorescence emission properties. The synthesized sensor is very efficient for onsite detection of Al^{3+} and Zn^{2+} ions by a paper strip test which can be applicable in analytical chemistry. In a biological pH medium, H_2L is most effective for the detection of these cations indicating the ability of sensing in biological systems. It has a low detection limit of 2.24×10^{-7} M and 0.41×10^{-7} M for Al^{3+} and Zn^{2+} ions respectively. So, our synthesized probe is a suitable sensor for detection of Al^{3+} and Zn^{2+} ions even in the presence of other metal ions.

Experimental

Material and methods

2-Amino-4-methylphenol and 4-phenylphenol were purchased from Sigma Aldrich and used without further purification. All other reagents and solvents were purchased from commercial sources and used without any further purification.

Elemental analysis was carried out using a 2400 Series-II CHN analyzer, Perkin Elmer, USA. HRMS mass spectra were recorded on a Waters (Xevo G2 Q-TOF) mass spectrometer. Infrared spectra were taken on a RX-1 Perkin Elmer spectrophotometer with samples prepared as KBr pellets. Electronic spectral studies were performed on a Perkin Elmer Lambda 25 spectrophotometer. Luminescence properties were measured using a Shimadzu RF-6000 fluorescence spectrophotometer at room temperature (298 K). NMR spectra were recorded using a Bruker (AC) 400 MHz FTNMR spectrometer of ~0.05 M solutions of the compounds in DMSO-d_6.

Synthesis of 4-hydroxy-[1,1′-biphenyl]-3-carbaldehyde

4-Phenylphenol (0.34 g, 2 mmol) is dissolved in 10 mL of trifluoroacetic acid. Hexamethylenetetraamine (0.28 g, 2 mmol) is added to the solution and refluxed at 90–100 °C for 6 h. After that the mixture is cooled to room temperature, and stirred in 30 mL 6 N HCl solution for 20 minutes. The product is separated by extraction with dry DCM solvent and purified by column chromatography. The prepared carbaldehyde is characterized by ^{1}H NMR spectroscopy. Yield: (0.32 g) 81%.

Synthesis of the probe 3-(((2-hydroxy-4-methylphenyl)imino)-methyl)-[1,1′-biphenyl]-4-ol (H_2L)

4-Hydroxy-[1,1′-biphenyl]-3-carbaldehyde (0.2 g, 1 mmol) is dissolved in 15 mL of ethanol in a round bottom flask.
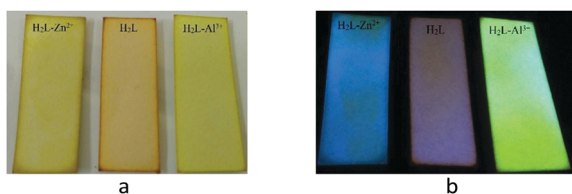

Fig. 12 Photographs of paper strips containing H_2L in the presence and absence of Al^{3+} and Zn^{2+} ions (a) in ambient light and (b) under UV light.

2-Amino-5-methylphenol (0.12 g, 1 mmol) is added to it and refluxed for 6 h. A shiny precipitate appears which is filtered, dried and collected. Yield: (0.27 g) 90%.

Elemental analysis. Anal. calcd for $C_{20}H_{17}NO_2$, C, 79.19%; H, 5.65%; N, 4.62%; found C, 79.13%; H, 5.70%; N, 4.68%.

IR (cm^{-1}, KBr). ν(C=N) 1610.21, ν(O–H) 3411.19, ν(N–H) 3026.57, ν(C=O) 1704.53.

^{1}H NMR (400 MHz, DMSO-d$_6$). δ (ppm): 2.24 (s, 3H), 6.84 (d, J = 8.07 Hz, 1H), 6.93 (d, J = 7.41 Hz, 1H), 7.0 (d, J = 8.49 Hz, 1H), 7.19 (s, 1H), 7.32 (d, J = 7.17 Hz, 1H), 7.44 (t, J = 7.38 Hz, 2H), 7.66 (m, 3H), 7.95 (s, 1H), 9.04 (s, 1H), 9.52 (s, 1H), 13.87 (s, 1H).

^{13}C NMR (400 MHz, DMSO-d$_6$). δ (ppm): 163.43, 160.04, 147.709, 139.96, 135.32, 132.85, 132.33, 130.92, 130.48, 129.38, 128.90, 127.07, 126.60, 119.44, 118.82, 117.73, 115.81, 77.45, 77.02, 76.60, and 20.64.

HRMS. MS-ES$^+$ (m/z): [M + H]$^+$: calculated: 304.1333, found: 304.0796.

UV-vis study

For this study, stock solutions of the receptor and the other ions were prepared separately. The receptor solution (20 μM) in [(CH$_3$OH/H$_2$O), 4 : 1, v/v, pH = 7.2] (at 25 °C) was prepared using a HEPES buffered solution of deionized water. Various metal ion solutions are prepared on the order of 40 μM using their chloride salt in deionised water. Fluoride solution was prepared using ammonium fluoride salt in deionized water. Other anion solutions were also prepared seperately on the same order as the cation, using their sodium salt in deionized water. For the UV-vis titration, solutions of various concentrations of the receptor and ions were prepared individually and spectra were taken.

Fluorescence study

For fluorescence titration, the solutions of the receptor and the ions were prepared in the same concentration and with the same procedure as used for the UV-vis study. Solutions of various concentrations of host and guest were prepared separately and emission spectra were recorded (λ_{ex} = 400 nm, excitation slit = 5.0 and emission slit = 5.0).

For the competition study, emission spectra of the receptor with Al^{3+} and Zn^{2+} were recorded individually in the presence of other cations. Fluorescence titrations of the H$_2$L–Al^{3+} and the H$_2$L–Zn^{2+} complex were also performed using F$^-$ (40 μM) and EDTA (40 μM) respectively.

Job plot analysis

Job plots were performed using fluorescence emission measurements. For Al^{3+}, a series of solutions with various concentrations of the receptor and metal ions have been prepared using H$_2$L (10 μm) and Al^{3+} (10 μm) in such a way that the total volume for each solution become equal (5 mL). Solutions are prepared in CH$_3$OH–H$_2$O (4 : 1, v/v) solvent at pH = 7.2 using HEPES buffer. The fluorescence emission of each solution was measured upon excitation at 400 nm. $\Delta I \cdot X_h$ versus X_h was plotted where ΔI is the change in emission intensity during titration and X_h is the mole fraction of host in the solution.

Conflicts of interest

There are no conflicts to declare.

Acknowledgements

References

1 B. Valeur and I. Leray, *Coord. Chem. Rev.*, 2000, **205**, 3–40.

2 J. P. Desvergne and A. W. Czarnik, *Chemosensors of Ion and Molecule Recognition*, NATO Science Series, Series C: Mathematical and Physical Sciences, Kluwer Academic, London, 1997.

3 Y. Li., C. Liao, S. Huang, H. Xu, B. Zheng, J. Du and D. Xiao, *RSC Adv.*, 2016, **6**, 25420–25426.

4 N. Roy, A. Dutta, P. Mondal, P. C. Paul and T. S. Singh, *J. Lumin.*, 2015, **165**, 167–173.

5 (*a*) D. Sarkar, P. Ghosh, S. Gharami, T. K. Mondal and N. Murmu, *Sens. Actuators, B*, 2017, **242**, 338–346; (*b*) M. Mukherjee, S. Pal, S. Lohar, B. Sen, S. Sen, S. Banerjee, S. Banerjee and P. Chattopadhyay, *Analyst*, 2014, **139**, 4828; (*c*) J. Sun, Z. Liu, Y. Wang, S. Xiao, M. Pei, X. Zhao and G. Zhang, *RSC Adv.*, 2015, **5**, 100873.

6 L. Ma, K. Liu, M. Yin, J. Chang, Y. Geng and K. Pan, *Sens. Actuators, B*, 2017, **238**, 120–127.

7 R. Bhowmick, A. S. M. Islam, A. Katarkar, K. Chaudhuri and M. Ali, *Analyst*, 2016, **141**, 225–235.

8 R. Vikneswaran, M. S. Syafiq, N. E. Eltayeb, M. N. Kamaruddin, S. Ramesh and R. Yahya, *Spectrochim. Acta, Part A*, 2015, **150**, 175–180.

9 J. Sivamani, V. Sadhasivam and A. Siva, *Sens. Actuators, B*, 2017, **246**, 108–117.

10 A. Patil, A. P. Ware, S. Bhand, D. Chakrovarty, R. Gonnade, S. S. Pingale and S. S. Gawali, *J. Mol. Struct.*, 2016, **1114**, 132–143.

11 L. Li, S. Yun, Z. Y. Hui, M. Lan, Z. Xi, C. Redshaw and W. Gang, *Sens. Actuators, B*, 2016, **226**, 279–288.

12 D. Shi, M. Ni, J. Luo, M. Akashi, X. Liua and M. Chen, *Analyst*, 2015, **140**, 1306–1313.

13 T. D. Giaccoa, R. Germania, F. Purgatorioa and M. Tiecco, *J. Photochem. Photobiol., A*, 2017, **345**, 74–79.

14 F. C. Liang, Y. L. Luo, C. C. Kuo, B. Y. Chen, C. J. Cho, F. J. Lin, Y. Y. Yu and R. Borsali, *Polymer*, 2017, **9**, 136.

15 S. Mohandoss, J. Sivakamavalli, B. Vaseeharanb and T. Stalin, *Sens. Actuators, B*, 2016, **234**, 300–315.

16 G. H. Robinson, *Chem. Eng. News*, 2003, **81**, 54–55.

17 S. Nandi and D. Das, *ACS Sens.*, 2016, **1**, 81–87.

18 C. Exley, *J. Inorg. Biochem.*, 2005, **99**, 1747–1928.

19 T. P. Flaten and M. Ødegård, *Food Chem. Toxicol.*, 1988, **26**, 959–960.

20 R. A. Yokel, *NeuroToxicology*, 2000, **21**, 813–828.

21 J. Ren and H. Tian, *Sensors*, 2007, **7**, 3166–3178.

22 S. H. Kim, H. S. Choi, J. Kim, S. J. Lee, D. T. Quang and J. S. Kim, *Org. Lett.*, 2010, **12**, 560–563.

23 (*a*) G. D. Fasman, *Coord. Chem. Rev.*, 1996, **149**, 125–165; (*b*) S. Pal, B. Sen, M. Mukherjee, M. Patra, S. Lahiri and P. Chattopadhyay, *RSC Adv.*, 2015, **5**, 72508.

24 T. P. Flaten, *Brain Res. Bull.*, 2001, **55**, 187–196.

25 M. Baral, S. K. Sahoo and B. K. Kanungo, *J. Inorg. Biochem.*, 2008, **102**, 1581–1588.

26 C. Exley, A. Begum, M. P. Woolley and R. N. Bloor, *Am. J. Med.*, 2006, **119**, 276 e9–276 e11.

27 Z. Krejpcio and R. W. Wojciak, *Pol. J. Environ. Stud.*, 2002, **11**, 251–254.

28 J. Barcelo and C. Poschenrieder, *Environ. Exp. Bot.*, 2002, **48**, 75–92.

29 T. Han, X. Feng, B. Tong, J. Shi, L. Chen, J. Zhi and Y. Dong, *Chem. Commun.*, 2012, **48**, 416–418.

30 J. M. Berg and Y. G. Shi, *Science*, 1996, **271**, 1081–1085.

31 B. L. Vallee and D. S. Auld, *Acc. Chem. Res.*, 1993, **26**, 543–551.

32 C. J. Frederickson, S. W. Suh, D. Silva, C. J. Frederickson and R. B. Thompson, *J. Nutr.*, 2000, **130**, 1471S–1483S.

33 E. L. Que, D. W. Domaille and C. J. Chang, *Chem. Rev.*, 2008, **108**, 1517–1549.

34 A. I. Bush, W. H. Pettingell, M. D. Paradis and R. E. Tanzi, *J. Biol. Chem.*, 1994, **269**, 12152–12158.

35 E. V. Stelmashook, N. K. Isaev, E. E. Genrikhs, G. A. Amelkina, L. G. Khaspekov, V. G. Skrebitsky and S. N. Illarioshkin, *Biochemistry*, 2014, **79**, 391.

36 C. D. Berdanier, J. T. Dwyer and E. B. Feldman, in *Handbook of Nutrition and Food*, ed. Nielsen, F. H., CRC Press, Boca Raton, FL, 2nd edn, 2007; ch. 8, p. 166.

37 G. Fosmire, *Am. J. Clin. Nutr.*, 1990, **51**, 225–227.

38 C. R. Cooper, N. Spencer and T. D. James, *Chem. Commun.*, 1998, 1365–1366.

39 C. B. Black, B. Andrioletti, A. C. Try, C. Ruiperez and J. L. Sessler, *J. Am. Chem. Soc.*, 1999, **121**, 10438–10439.

40 L. S. Kaminsky, M. C. Mahoney, J. Leach, J. Melius and M. Jo Miller, *Crit. Rev. Oral Biol. Med.*, 1990, **1**, 261–281.

41 D. Browne, H. Whelton and D. O'Mullane, *J. Dent.*, 2005, **33**, 177–186.

42 R. Schwarzenbach, B. I. Escher, K. Fenner, T. B. Hofstetter, C. A. Johnson, U. von Gunten and B. Wehrli, *Science*, 2006, **313**, 1072–1077.

43 S. Jagtap, M. K. Yenkie, N. Labhsetwar and S. Rayalu, *Chem. Rev.*, 2012, **112**, 2454–2466.

44 Y. Fu, Y. Tu, C. Fan, C. Zheng, G. Liu and S. Pu, *New J. Chem.*, 2016, **40**, 8579.